Received: 12 August 2021 | Revised: 25 November 2021 | Accepted: 9 December 2021

DOI: 10.1111/mpp.13178

Molecular Plant Pathology WILEY

TECHNICAL ADVANCE

Highly efficient genome editing in *Xanthomonas oryzae* pv. *oryzae* through repurposing the endogenous type I-C CRISPR-Cas system

Dandan Jiang[1,2] | **Dandan Zhang**[1] | **Shengnan Li**[1] | **Yueting Liang**[1,2] | **Qianwei Zhang**[1,2] | **Xu Qin**[1,2] | **Jinlan Gao**[1] | **Jin-Long Qiu**[1,2]

[1]State Key Laboratory of Plant Genomics, Institute of Microbiology, Chinese Academy of Sciences, Beijing, China

[2]CAS Center for Excellence in Biotic Interactions, University of Chinese Academy of Sciences, Beijing, China

Correspondence
Jin-Long Qiu, State Key Laboratory of Plant Genomics, Institute of Microbiology, Chinese Academy of Sciences, Beijing 100101, China.
Email: qiujl@im.ac.cn

Funding information
Strategic Priority Research Program of the Chinese Academy of Sciences, Grant/Award Number: XDA24020101 and XDPB16; National Natural Science Foundation of China, Grant/Award Number: 32001891 and 31901868

Abstract

Efficient and modular genome editing technologies that manipulate the genome of bacterial pathogens will facilitate the study of pathogenesis mechanisms. However, such methods are yet to be established for *Xanthomonas oryzae* pv. *oryzae* (Xoo), the causal agent of rice bacterial blight. We identified a single type I-C CRISPR-Cas system in the Xoo genome and leveraged this endogenous defence system for high-efficiency genome editing in Xoo. Specifically, we developed plasmid components carrying a mini-CRISPR array, donor DNA, and a phage-derived recombination system to enable the efficient and programmable genome editing of precise deletions, insertions, base substitutions, and gene replacements. Furthermore, the type I-C CRISPR-Cas system of Xoo cleaves target DNA unidirectionally, and this can be harnessed to generate large genomic deletions up to 212 kb efficiently. Therefore, the genome-editing strategy we have developed can serve as an excellent tool for functional genomics of Xoo, and should also be applicable to other CRISPR-harbouring bacterial plant pathogens.

KEYWORDS
bacterial pathogen, genome editing, rice, type I-C CRISPR-Cas system, *Xanthomonas oryzae* pv. *oryzae*

1 | INTRODUCTION

Rice (*Oryza sativa*) is a major staple crop in the world. Bacterial blight caused by *Xanthomonas oryzae* pv. *oryzae* (Xoo) is one of the major diseases threatening rice production (Joshi et al., 2020). Xoo enters the rice leaf through wounds or hydathodes at the leaf tip and margin, then moves to and spreads through the xylem vessels (Mew et al., 1993). Ongoing growth of Xoo fills these vessels, and leads to lesions expanding lengthwise on leaf blades, ultimately killing the leaves (Niño-Liu et al., 2006). Bacterial blight causes yield losses ranging from 20% to 30%, sometimes reaching levels of 50%, in tropical Asian countries and in other areas, such as Africa (Jiang et al., 2020; Liu et al., 2014; Verdier et al., 2012). Importantly, the rice–Xoo interaction is a fundamental model system used widely to study plant innate immunity in monocots (Chen & Ronald, 2011).

Genetic manipulation of Xoo has greatly expanded our understanding of the molecular basis of its pathogenicity. Two methods are commonly used for gene disruption in Xoo; one is transposon-based

Dandan Jiang, Dandan Zhang, and Shengnan Li contributed equally to this work.

mutagenesis (Wang et al., 2008) and the other is targeted mutagenesis based on homologous recombination. The Tn*5* transposon is an efficient tool for insertional mutagenesis in Xoo (Sun et al., 2003), which can result in gene knockouts or affect the expression of genes surrounding the insertion sites, leading to various phenotypic perturbations. The targeted mutagenesis strategy typically requires two rounds of selection to identify bacterial cells with double-crossover events that result in either the generation of seamless mutations or reversion to wild type (Hmelo et al., 2015; Schäfer et al., 1994). However, transposon insertion lacks site specificity while double-crossover-mediated homologous recombination is relatively inefficient. Moreover, both approaches require selective markers for selection and enrichment of the genomic perturbation (Sun et al., 2003; Zou et al., 2011).

Recently, CRISPR-Cas systems have been developed as powerful tools for targeted genome modifications (Anzalone et al., 2020; Arroyo-Olarte et al., 2021). CRISPR-Cas systems are native to most archaea and more than 40% of bacterial species, and function as defensive systems conferring adaptive immunity to viruses and plasmids (Grissa et al., 2007; Kessler et al., 2004; Makarova et al., 2015, 2018). CRISPR-Cas systems can be broadly divided into two classes. Class 1 is composed of type I, III, and IV CRISPR-Cas systems, characterized by multi-subunit effector complexes, whereas class 2 is composed of type II, V, and VI CRISPR-Cas systems, which are characterized by single-protein effectors (Makarova et al., 2018). Although nearly 90% of CRISPR-Cas systems belong to class 1 (Makarova et al., 2015), the class 2 single-effector nucleases, such as Cas9 and Cas12a, have been most widely adopted as genome-editing tools in various organisms, including bacteria (Arroyo-Olarte et al., 2021), presumably due to their simplicity.

CRISPR-based genome editing in most bacteria is distinct due to their lack of a nonhomologous end-joining repair pathway (Rocha et al., 2005; Vento et al., 2019). CRISPR-induced double-strand break is often lethal in bacteria, and this can be used as an alternative counterselection for edited cells without the need for selective markers (Arroyo-Olarte et al., 2021; Jiang et al., 2013). To date, Cas9 and Cas12a have been successfully used in a few bacterial species, and among them, some are pathogenic bacteria (Hong et al., 2018; Penewit et al., 2018). The application of these editing systems in bacteria is not as widespread as in eukaryotes potentially due to bacterial toxicity caused by the heterologous expression of Cas9 or Cas12a, the requirement for time-consuming optimizations of these editing systems in each bacterial strain, and the low efficiency of transformation of editing components into certain bacteria (Arroyo-Olarte et al., 2021; Xu et al., 2021). Therefore, there is a need to explore the use of different CRISPR systems to achieve efficient genome editing in diverse bacteria, especially transformation-recalcitrant bacterial species.

Because nearly half of all bacterial species encode endogenous CRISPR-Cas systems (Makarova et al., 2018), harnessing these native CRISPR systems for genome editing can avoid additional toxicity caused by any expression of exogenous Cas nucleases. Furthermore, using endogenous components helps with limiting the need to transform additional *cas* genes. Native type I CRISPR systems have been repurposed for genome editing in several bacterial species, such as the use of subtype I-A in *Sulfolobus islandicus* and *Heliobacterium modesticaldum*, subtype I-B systems in *Clostridium pasteurianum* and *Haloarcula hispanica*, subtype I-E in *Lactobacillus crispatus*, and subtype I-F in *Zymomonas mobilis* and *Pseudomonas aeruginosa* (Baker et al., 2019; Cheng et al., 2017; Li et al., 2016; Maikova et al., 2019; Pyne et al., 2016; Xu et al., 2019; Zheng et al., 2019). However, few CRISPR-Cas systems have been characterized, let alone repurposed for genome editing, in phytopathogenic bacteria (Todor et al., 2021).

In this work, we examined the use of an endogenous CRISPR-Cas system for efficient genome editing in Xoo. Analysis of the Xoo genome sequence revealed that Xoo contains a type I-C CRISPR-Cas locus. We first characterized the activity of this CRISPR-Cas system, and then repurposed it for genome editing using CRISPR arrays containing self-targeting spacers. In the presence of DNA repair templates and a λ-Red recombination system, high efficiency genome editing with various outcomes was achieved in Xoo. Our work reveals an efficient approach to explore functional genomics in Xoo, while also providing a technical framework applicable to other bacteria, especially plant pathogens, that harbour native functional CRISPR-Cas loci.

2 | RESULTS

2.1 | Identification of a single CRISPR-Cas locus in the genome of Xoo

The genome sequence of Xoo strain PXO99^{A} was analysed using CRISPRCasFinder (Grissa et al., 2007) and a single CRISPR-Cas locus was identified (Figure 1a). Based on its features, this native CRISPR-Cas system belongs to subtype I-C, members of which are made up of the type I CRISPR-Cas signature gene *cas3*, together with *cas5d*, *cas8c*, and *cas7*, altogether constituting the surveillance complex Cascade (CRISPR-associated complex for antiviral defence) (Makarova et al., 2018; Nam et al., 2012). Cas5d is also responsible for processing CRISPR RNA precursors (pre-crRNA) to generate mature crRNAs (Hochstrasser et al., 2016; Nam et al., 2012). The native CRISPR array contains 75 spacers separated by 31-nucleotide (nt) direct repeat sequences (5′-GTCGCGTCCTCACGGGCGCGTGG ATTGAAAC-3′). Based on the crRNA structure from other subtype I-C CRISPR systems (Hochstrasser et al., 2016), each mature crRNA in Xoo is predicted to be made up of a 5′ handle (11 nt), a spacer (33–37 nt), and a 3′ stem-loop (20 nt) (Figure 1b). RNA sequencing of Xoo cells revealed the expression of *cas* genes and the CRISPR array (Figure 1c), thus suggesting a functional endogenous type I-C CRISPR-Cas system.

2.2 | Characterization of the protospacer adjacent motif

A protospacer adjacent motif (PAM) is needed for target recognition by prokaryotic CRISPR defence systems (Mojica et al., 2009).

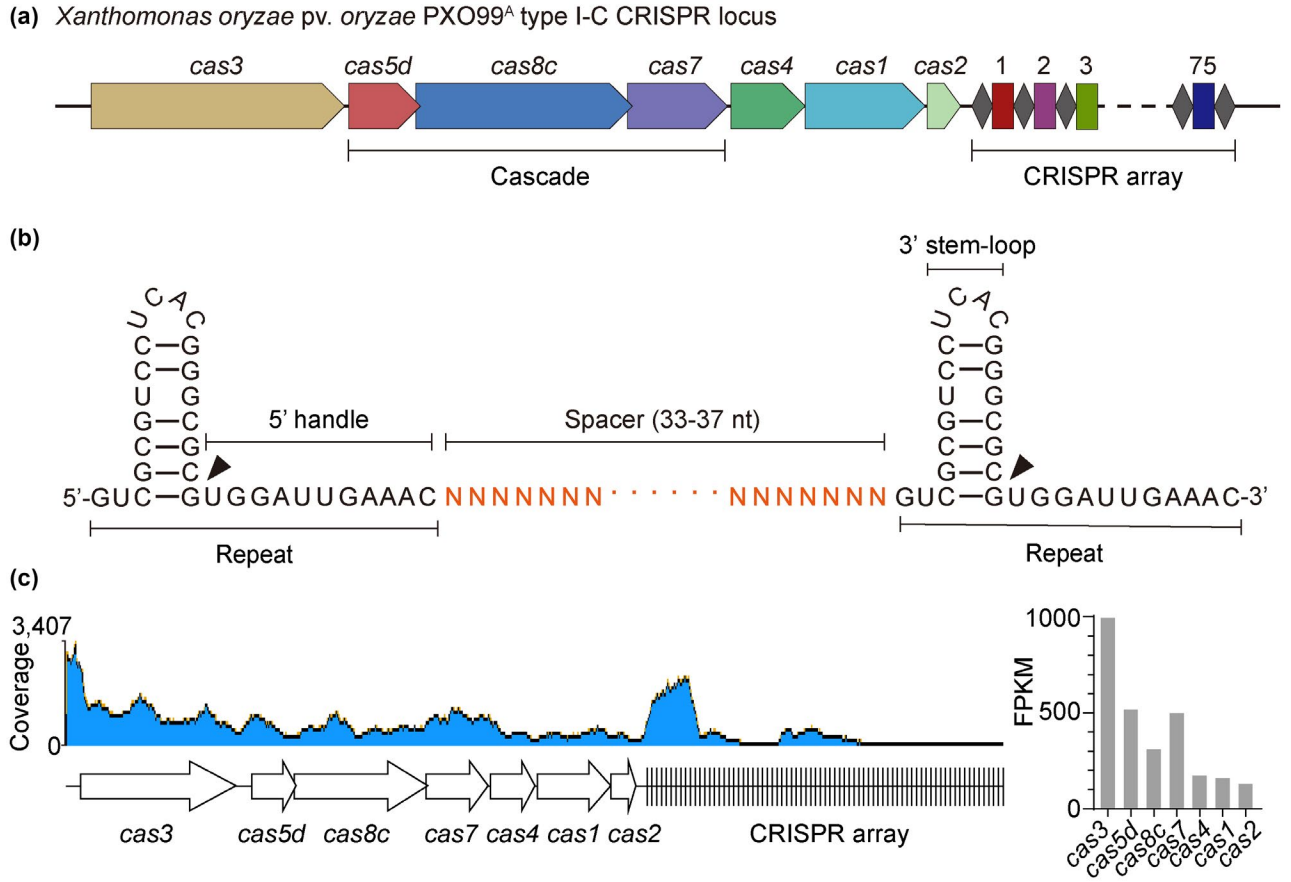

FIGURE 1 A single CRISPR-Cas locus in the genome of *Xanthomonas oryzae* pv. *oryzae* PXO99^A. (a) Schematic of the *cas* locus and the CRISPR array in the genome of PXO99^A. Diamonds represent conserved direct repeats. Rectangles in different colours represent different spacers, with the number of total spacers indicated above. (b) Schematic representation of the pre-crRNA transcript processed by Cas5d into mature crRNA. A mature crRNA is composed of a 11-nucleotide (nt) 5′ handle, a spacer consisting of 33–37 nt (orange), and a 20-nt 3′ stem-loop. The triangles indicate predicted cleavage sites. (c) RNA-Seq data showing the transcriptional profile of the type I-C CRISPR locus in PXO99^A (left panel). Gene expression values (fragments per kilobase per million reads, FPKM) for *cas* genes based on RNA-Seq data (right panel)

To characterize the PAM required by the type I-C system of Xoo, the native CRISPR array sequence was submitted to CRISPR Target (Biswas et al., 2013) with default parameters to search for foreign DNA sequences from phages and plasmids that matched with the corresponding spacer sequences. Consistent with a previous report (Martins et al., 2019), we identified 40 spacers with significant homology to phage sequences and seven spacers with homology to plasmid sequences, implying that this CRISPR-Cas system is implicated in adaptive immunity. Further analysis of the putative target sequences (protospacers) with WebLogo (Crooks et al., 2004) revealed a 5′-TTN-3′ PAM upstream of the protospacers for this type I-C CRISPR-Cas system (Figure 2a). A similar PAM is used by the type I-C CRISPR systems of *Bacillus halodurans* (Leenay et al., 2016) and *Legionella pneumophila* (Rao et al., 2016). In addition to the 5′-TTN-3′ PAM identified, other putative PAM sequences were also identified with relatively high confidence (Table S1).

To confirm the function of these putative PAM sequences, we performed a plasmid transformation interference assay using spacer 1 of the native CRISPR array (Pyne et al., 2016). The protospacer together with various triplets of 5′ putative PAM sequences were cloned into the vector pHM1 (Hopkins et al., 1992; Innes et al., 1988), and the resulting target plasmids were transformed into competent Xoo PXO99^A cells. As shown in Figure 2b, significant differences in transformation efficiency were observed with plasmids containing different PAMs. Plasmids containing PAMs 5′-TTA-3′, 5′-TTT-3′, 5′-TTC-3′, 5′-TTG-3′, and 5′-CTC-3′ yielded few colonies, whereas plasmids harbouring other PAMs and the control plasmid pHM1 transformed Xoo efficiently. Overall, the use of a 5′-TTN-3′ or 5′-CTC-3′ PAM led to growth of approximately 10,000-fold fewer transformants compared to the control plasmid (Figure 2b), confirming that these sequences were functional PAM sequences for the type I-C CRISPR-Cas system of Xoo.

2.3 | Repurposing the endogenous CRISPR-Cas system for gene editing in Xoo

Knowing that the CRISPR-Cas system in Xoo is functional and has high interference activity against plasmids with the appropriate PAM sequences and protospacer, we next repurposed this endogenous

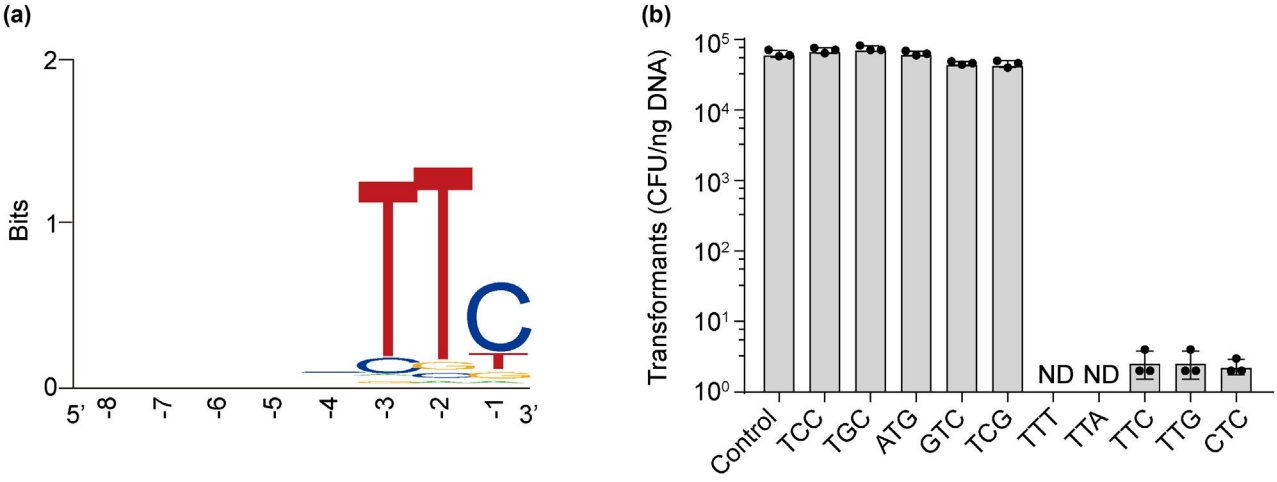

FIGURE 2 Functional protospacer adjacent motif (PAM) sequences for the type I-C CRISPR-Cas system. (a) PAMs were predicted for the type I-C CRISPR-Cas. The 5′-end flanking sequences of the potential protospacers matching the 75 spacers in the PXO99^A CRISPR array were imported into WebLogo for PAM prediction. (b) Validation of putative PAMs by plasmid transformation interference assay. Putative PAM sequences and protospacer 1 matched by spacer 1 in the CRISPR array were cloned into plasmid pHM1. Empty plasmid pHM1 was used as a control. The plasmids were transformed into PXO99^A. CFU, colony-forming units. ND, not detected. Error bars represent standard deviations, $n = 3$

system as a genome-editing tool for Xoo. We first set out to edit an *EGFP* gene on the pHM1 plasmid in PXO99$^A{}_{EGFP}$ cells (Zhang et al., 2019). To this end, we assembled an *EGFP*-targeting 34-nt spacer flanked by two 31-nt direct repeats into the pSEVA vector, yielding pSEVA-egfpT. We also designed a donor template consisting of homology 500-bp upstream and 500-bp downstream of the target region, which contains a premature stop codon in *EGFP* for early translation termination and in which the PAM sequence is mutated so any edited sequences can no longer be repeatedly targeted. The pSEVA-egfpTD plasmid was constructed by inserting sequences of the donor template into pSEVA-egfpT, and was then introduced into PXO99$^A{}_{EGFP}$ cells. We used the plasmid pHM1-EGFP as a reporter plasmid; after targeting by a crRNA, the plasmid will be degraded and thereby lead to loss of spectinomycin resistance in the bacterial cells (Figure S1a). If a repair donor template is provided, the bacterial cells can survive due to homologous recombination repair of the cut DNA (Figure S1b). As shown in Figure 3a, the number of colonies obtained on the plate by pSEVA-egfpTD transformation (17 ± 3 cfu/μg DNA) was moderately higher than that obtained with pSEVA-egfpT alone (6 ± 1 cfu/μg DNA), indicating Xoo strains do not support efficient homology-based recombination following induction of CRISPR-mediated double-strand DNA breaks. Therefore, we introduced the phage-derived recombination system λ-Red, which includes the *gam*, *beta*, and *exo* genes (Datsenko & Wanner, 2000; Jiang et al., 2015) under control of P_{araB} (Guzman et al., 1995), into the pHM1-EGFP vector, yielding pHM1-EGFP-λRed. When we transformed pSEVA-egfpTD into PXO99$^A{}_{EGFP\text{-}\lambda Red}$ cells, the number of transformants increased significantly (413 ± 63 cfu/μg DNA) (Figure 3a). These results indicate that the endogenous CRISPR-Cas system can be modularly reprogrammed with foreign-derived crRNA sequences and that heterologous recombinases can perform accurate and efficient gene editing in Xoo.

2.4 | Harnessing the native CRISPR-Cas system for editing of endogenous genes in Xoo

As the native type I-C CRISPR-Cas system is effective at editing heterologous genes on plasmids, we next explored its ability to edit endogenous genes. We chose *xanB2* (*PXO_03739*), which plays a key role in xanthomonadin biosynthesis and produces membrane-bound yellow pigments (Zhou et al., 2013), to target with our reprogrammed Cas system. A *xanB2* deletion mutant that fails to produce xanthomonadin exhibits a white colony phenotype (Zhou et al., 2013). We constructed a pSEVA-xanb2TD plasmid to carry a mini-CRISPR array targeting the *xanB2* gene and a repair donor consisting of homology 500 bp upstream and downstream of the target site to remove the entirety of the targeted gene (Figure 3b). These plasmids were introduced into Xoo competent cells but resulted in a very low number of transformants (Figure S2a). This result is in agreement with that obtained when editing the heterologous *EGFP* gene on plasmids (Figure 3a). Therefore, we constructed a helper λ-Red recombination system into the pHM1 vector, yielding pHM1-λRed (Figure 3b), and transformed this into Xoo to improve the frequency of homologous recombination. We ultimately used the resulting PXO99$^A{}_{\lambda Red}$ cells in all subsequent editing experiments. The pSEVA-xanb2TD plasmid was first transformed into PXO99$^A{}_{\lambda Red}$ cells, and we next observed that 99.5% ± 0.7% colonies exhibited a white phenotype, suggesting that they harboured the desired *xanB2* mutation (Figure 3c,d). Targeted DNA sequencing confirmed the presence of the expected *xanB2* deletion in the Xoo genome of white colonies (Figure S2b,c).

To demonstrate the versatility of our optimized editing approach in Xoo, we next chose to edit additional chromosomal locations. We chose to delete either the *detR* (detoxifying regulator) gene or the non-TAL effector *xopQ* gene (Figure S3a–c). Δ*detR* or Δ*xopQ* strains resulted in editing rates of 87.9% ± 1.9% and 98.3% ± 2.9%, respectively (Figure S3d,e).

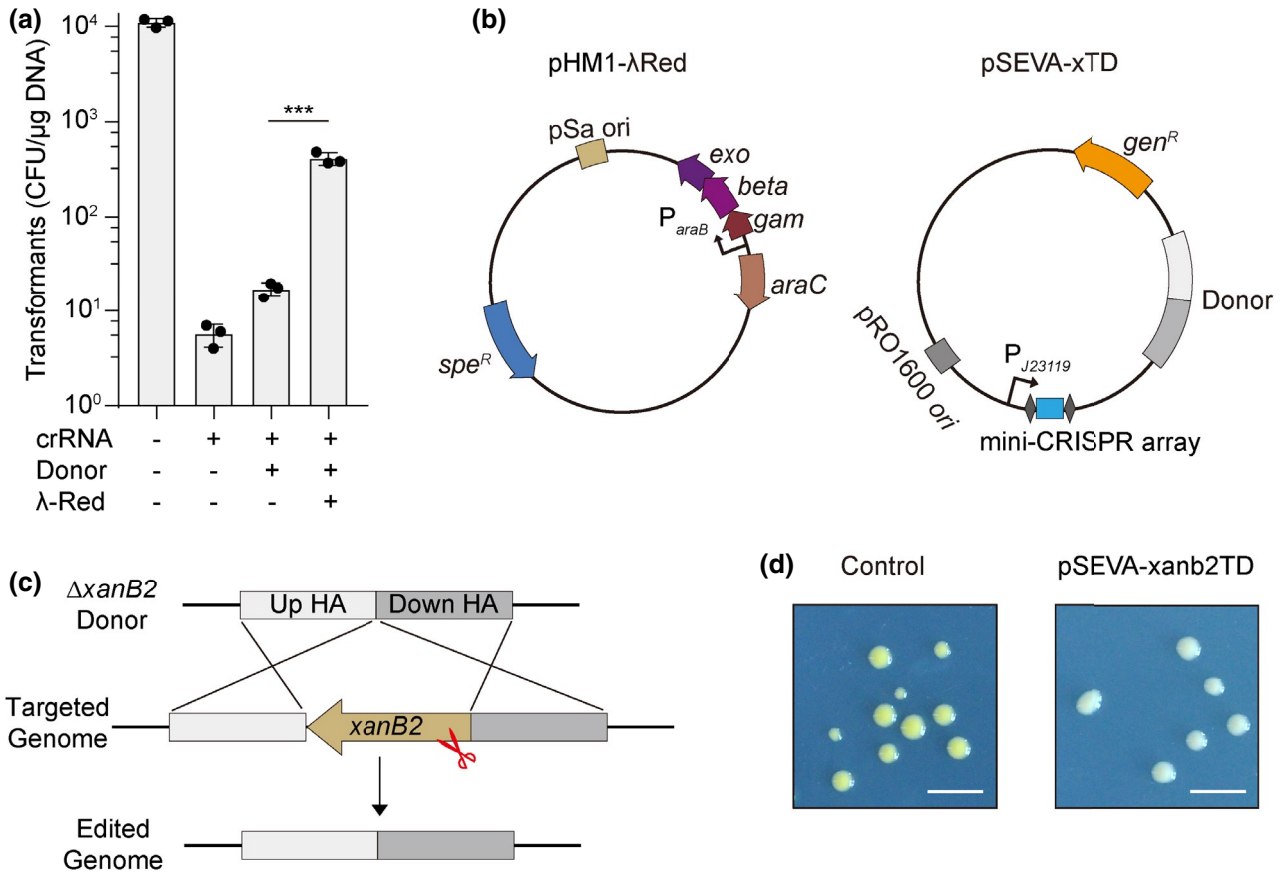

FIGURE 3 Genome editing achieved by repurposing the endogenous type I-C CRISPR-Cas system in *Xanthomonas oryzae* pv. *oryzae*. (a) Numbers of transformants were generated with the plasmids carrying different components for *EGFP* gene editing. Error bars represent standard deviations, $n = 3$. Statistical significance was determined by two-tailed Student's *t* tests (***$p < 0.001$). (b) Schematic map of the two plasmids used for genome editing by repurposing the endogenous CRISPR-Cas system. Plasmid pHM1-λRed contains an arabinose-inducible λ-Red system to improve recombination efficiency. Plasmid pSEVA-xTD contains a mini-CRISPR array encoding the crRNA that targets gene "x" and the donor sequence consisting of the upstream and downstream homologous arms of the target gene. (c) The schematic diagram for *xanB2* gene deletion by the repurposed type I-C CRISPR-Cas system. The cleavage site of the CRISPR-Cas system is indicated by the red scissors. HA, homologous arm. (d) Colonies obtained after pSEVA-xanb2TD for *xanB2* gene deletion was transformed into PXO99^{A} harbouring pHM1-λRed. Plasmid pSEVA-NT expressing nontargetable crRNA used as a control. Scale bar: 0.5 cm

Because the *detR* gene functions in extracellular polysaccharide (EPS) synthesis, Δ*detR* colonies appeared drier and smaller than those of wild-type cells on peptone sucrose agar (PSA) medium (Figure S4a), which is consistent with a previous report (Nguyen et al., 2016).

To assess the impact of donor size on genome-editing efficiency, we constructed a new donor plasmid in pSEVA by replacing the upstream and downstream 500-bp homologous arms with 1000-bp homologous arms. Although the 1000-bp homologous arms greatly increased the transformation efficiency, the editing rate remained comparable (Figure S3d,e). Therefore, longer repair arms can increase transformant counts but 500-bp repair arms are sufficient for optimal genome editing in Xoo.

2.5 | Diverse editing outcomes achieved by repurposing the native CRISPR-Cas system in Xoo

We next explored the diversity of editing outcomes that could be achieved by repurposing the endogenous CRISPR-Cas system. Point mutations in the coding region of a gene that result in amino acid changes can alter the activity of an enzyme, which is orthogonal to the study of simple protein knockouts. A two-nucleotide change (CCG to TTG) in *xanB2* yields an amino acid substitution (P169L) that significantly affects xanthomonadin biosynthesis (Zhou et al., 2013). To explore the capability of our editing system in generating programmable base substitutions, we introduced a two-base substitution into the repair template and cloned the resulting sequence into the pSEVA plasmid carrying a 34-nt spacer targeting *xanB2* (Figure 4a). After transforming this construct into PXO99$^{A}_{\lambda Red}$ cells, we observed that 74.4% ± 3.4% transformant colonies obtained were white (Figure 4b). Targeted DNA sequencing further confirmed the presence of the desired two-base substitution in the *xanB2* gene of white transformants (Figure 4c).

To further evaluate our editing method to generate precise gene insertions, we selected a target site between *PXO_00827* and *PXO_00828* in Xoo. We designed a repair template containing *EGFP* under the control of a *lacZ* promoter flanked by 500-bp homologous arms and cloned this resulting sequence into pSEVA (Figure 4d). The

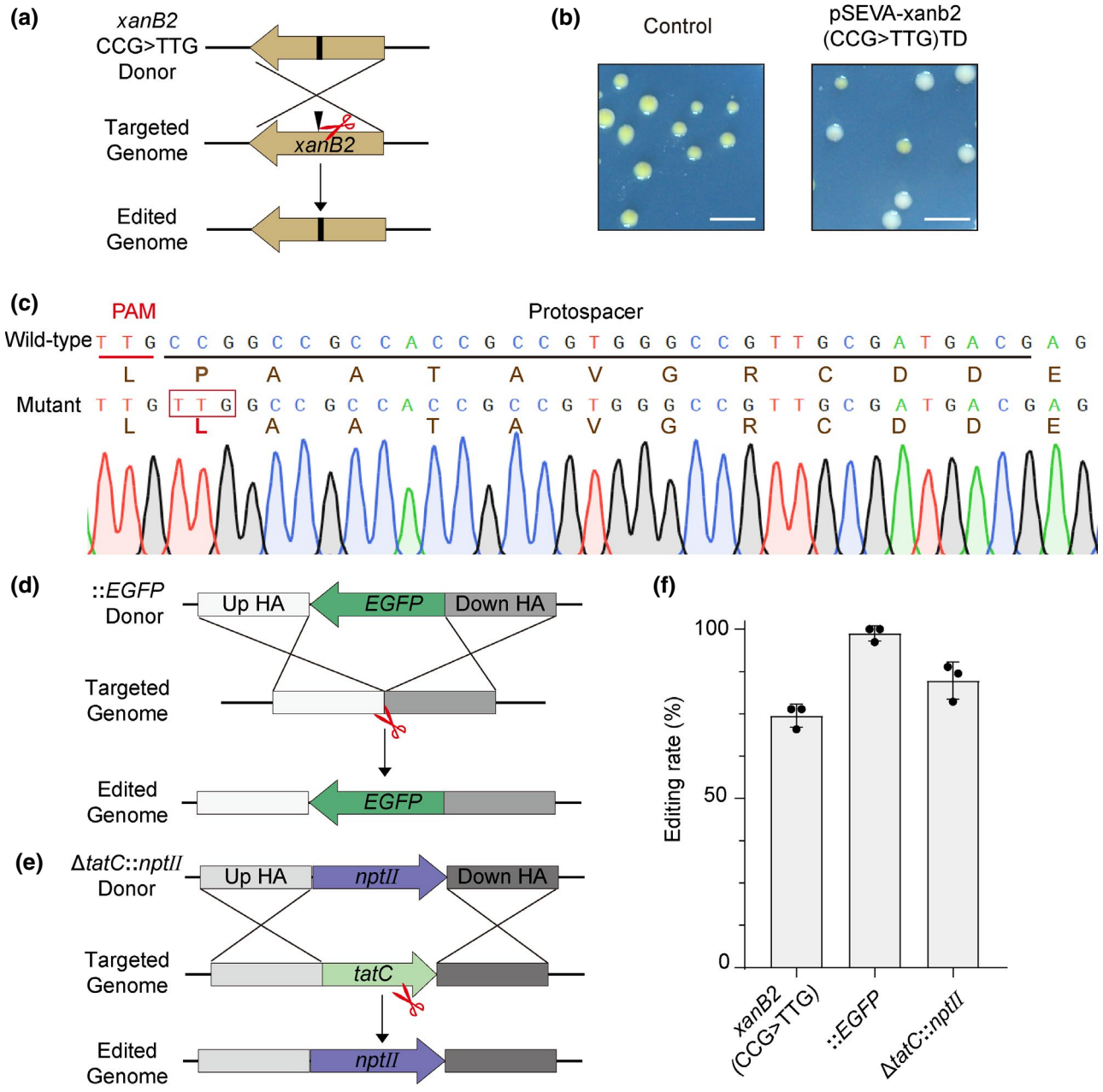

FIGURE 4 Base substitutions, targeted gene insertion, and gene replacement achieved by harnessing the native CRISPR-Cas system in *Xanthomonas oryzae* pv. *oryzae*. (a) Schematic diagram for base substitutions resulting in the P196L amino-acid change in *xanB2* by repurposing the endogenous type I-C CRISPR-Cas system. The mutation site in *xanB2* is indicated by a black rectangle. The cleavage site of the endogenous CRISPR-Cas system is indicated by the red scissors. (b) Colonies obtained after pSEVA-xanb2(CCG>TTG)TD transformed into PXO99^{A} harbouring pHM1-λRed for base substitutions. Plasmid expressing nontargetable crRNA used as a control. Scale bar: 0.5 cm. (c) DNA sequencing result confirmed the two-nucleotide substitutions at the *xanB2* target site. (d, e) Schematic diagram for *EGFP* insertion (d) and gene replacement (e) by repurposing the endogenous type I-C CRISPR-Cas system. The cleavage site of the endogenous CRISPR-Cas system is indicated by the red scissors. HA, homologous arm. (f) Editing rate of the diverse genome-editing outcomes given by the percentages of positive colonies harbouring the desired mutations. Error bars represent standard deviations, $n = 3$

resulting transformants were examined with PCR amplification and DNA sequencing to confirm the intended insertions (c.1 kb) at an editing rate of 98.7% ± 2.2% (Figure S5a,c).

We also explored the ability to result in gene replacements using our optimized editing method. We targeted *tatC*, which encodes a vital component of the twin-arginine translocation system, to be replaced with the exogenous *nptII* gene encoding a kanamycin resistance protein, neomycin phosphotransferase (Figure 4e). The donor plasmid was generated by inserting a c.1 kb *nptII*-encoding cassette between 500-bp homology arms together with a spacer that targets *tatC*. Transformants were selected with kanamycin and sequenced to confirm the desired genome replacement in the target region. A larger PCR product of c.1.8 kb was amplified in 84.8% ± 5.5% transformants, which corresponds to

the length as predicted following successful gene replacement, and the programmed edit was further confirmed by DNA sequencing (Figure S5b,d).

Overall, we achieved editing rates of base substitutions, gene insertion, and gene replacement of 74.4% ± 3.4%, 98.7% ± 2.2%, and 84.8% ± 5.5%, respectively (Figure 4f). These results show that various chromosomal loci can be targeted modularly and efficiently using the endogenous type I-C system in Xoo to generate a variety of genome-edited outcomes, including gene deletion, base substitutions, insertion, and gene replacement.

2.6 | Large genomic deletions generated by harnessing the type I-C CRISPR-Cas system

In type I CRISPR systems, the helicase-nuclease Cas3 degrades target DNA processively, and this unique feature has been developed for large genomic deletions in eukaryotes and prokaryotes (Dolan et al., 2019; Zheng et al., 2019). Thus, we tested the ability of the native type I-C system from Xoo to delete a 16-kb *gum* gene cluster, which consists of 14 open reading frames encoding proteins involved in xanthan biosynthesis and pathogenicity of Xoo (Katzen et al., 1998; Kim et al., 2009; Yoon & Cho, 2007). After transforming plasmids that express the *gumH*-targeting crRNA #1 and carry a donor with c.1 kb homologous flanking regions upstream and downstream of the *gum* gene cluster, we obtained an average of 57 ± 7 cfu/μg DNA (Figure 5a,b). The transformants obtained formed small and dry colonies (Figure S4b), which is consistent with the phenotype of xanthan absence (Yoon & Cho, 2007).

Cas3 is a 3′–5′ single-strand DNA helicase-nuclease (Sinkunas et al., 2011). Previous reports showed that Cas3 from type I-C and type I-E CRISPR systems translocates unidirectionally toward the PAM-proximal direction to cleave target DNA (Dolan et al., 2019; Mulepati & Bailey, 2013; Nimkar & Anand, 2020; Sinkunas et al., 2013). We next sought to evaluate the processive nature of the Cas3 enzyme in the Xoo type I-C CRISPR system. To this end, we designed two pairs of crRNAs to target the *gum* gene cluster. One pair of crRNAs, *gum* crRNA #2A and #2B, was selected, whose PAM-proximal direction is towards the gene cluster (Figure 5a). The other pair consisted of crRNAs *gum* crRNA #3A and #3B, whose PAM-proximal direction is opposite to the gene cluster (Figure 5a). When we transformed plasmids carrying the corresponding crRNAs into $PXO99^{A}_{\lambda Red}$ cells, the number of transformants generated with *gum* crRNA #2A and #2B (270 ± 4 cfu/μg DNA) was considerably more than when delivering *gum* crRNA #3A and #3B (15 ± 9 cfu/μg DNA) (Figure 5b). We speculated that the *gum* crRNA #2A and #2B guided the type I-C CRISPR system to cleave towards the *gum* cluster, keeping the homologous arm sequences intact and thereby facilitating recombination with repair donors. In contrast, the *gum* crRNA #3A and #3B guided the type I-C CRISPR system to cleave towards the homologous arm sequences, which would limit successful repair mediated by homologous recombination. Interestingly, the number of transformants with *gum* crRNA #2A and #2B was also much higher than that obtained with the single *gum* crRNA #1 (Figure 5a,b). Nonetheless, the editing rate of these combinations of crRNAs remained at a comparatively high level (Figure 5b). PCR amplification of the genomic DNA revealed that most transformants had our desired deletion (Figure 5b,c), which was further confirmed by DNA sequencing (Figure 5d).

We further tested this phenomenon at the *hrp* gene cluster, which encodes components of the type III secretion system and is essential for the pathogenicity of Xoo (Cornelis, 2006; Zhu et al., 2000). Using a similar procedure as described above, we obtained more transformants generated when delivering *hrp* crRNA #2A and #2B (293 ± 6 cfu/μg DNA), whose PAM-proximal direction is towards the cluster, than when delivering *hrp* crRNA #3A and #3B (17 ± 5 cfu/μg DNA), which targets an opposite PAM-proximal direction, or the single *hrp* crRNA #1 (166 ± 5 cfu/μg DNA) (Figure 5e). All randomly picked colonies lost the 28-kb *hrp* gene cluster when analysed by PCR amplification and DNA sequencing (Figure 5e and Figure S6a,b). These data support that the Xoo type I-C CRISPR-Cas system primarily generates unidirectional deletions.

We then explored the generation of deletions exceeding the lengths of the *gum* and *hrp* gene clusters. The genome of the Xoo strain $PXO99^{A}$ contains a near-perfect 212 kb tandem repeat close to the replication terminus (Salzberg et al., 2008). We designed a pair of crRNAs that targets one copy of the 212 kb direct repeat for deletion (Figure 5f). This pair of crRNAs combined with the corresponding repair template generated a considerable number of transformants (175 ± 9 cfu/μg DNA), and PCR amplification and DNA sequencing confirmed the targeted genomic deletion in these transformants (Figure 5f and Figure S6c). Together, these data support that the Xoo type I-C system can induce large genomic deletions efficiently, and should provide a tool for exploring the function and essentiality of large segments of the genome.

To evaluate the pathogenicity of the Xoo Δ*hrp*, Δ*gum*, and Δ212 kb mutants, leaves of the rice cultivar Nipponbare were inoculated with these strains using the leaf-clipping method. Both the Δ*hrp* and Δ*gum* mutants lost the ability to cause disease symptoms in the susceptible rice leaves, but not the Δ212 kb mutant (Figure S7).

3 | DISCUSSION

Plant-pathogenic bacteria are widespread threats to global food production (Mansfield et al., 2012; Savary et al., 2019). Efficient genetic manipulation tools are needed to comprehensively understand the molecular mechanism of pathogenesis of these bacteria and their interactions with plants. In this study, we established an efficient genome-editing tool in Xoo by harnessing its endogenous type I-C CRISPR system.

The functionality of the endogenous type I-C CRISPR system in Xoo was supported by transcriptome data and plasmid transformation interference assay (Figures 1c and 2b). However, efficient genome editing could not be achieved by simply delivering a CRISPR

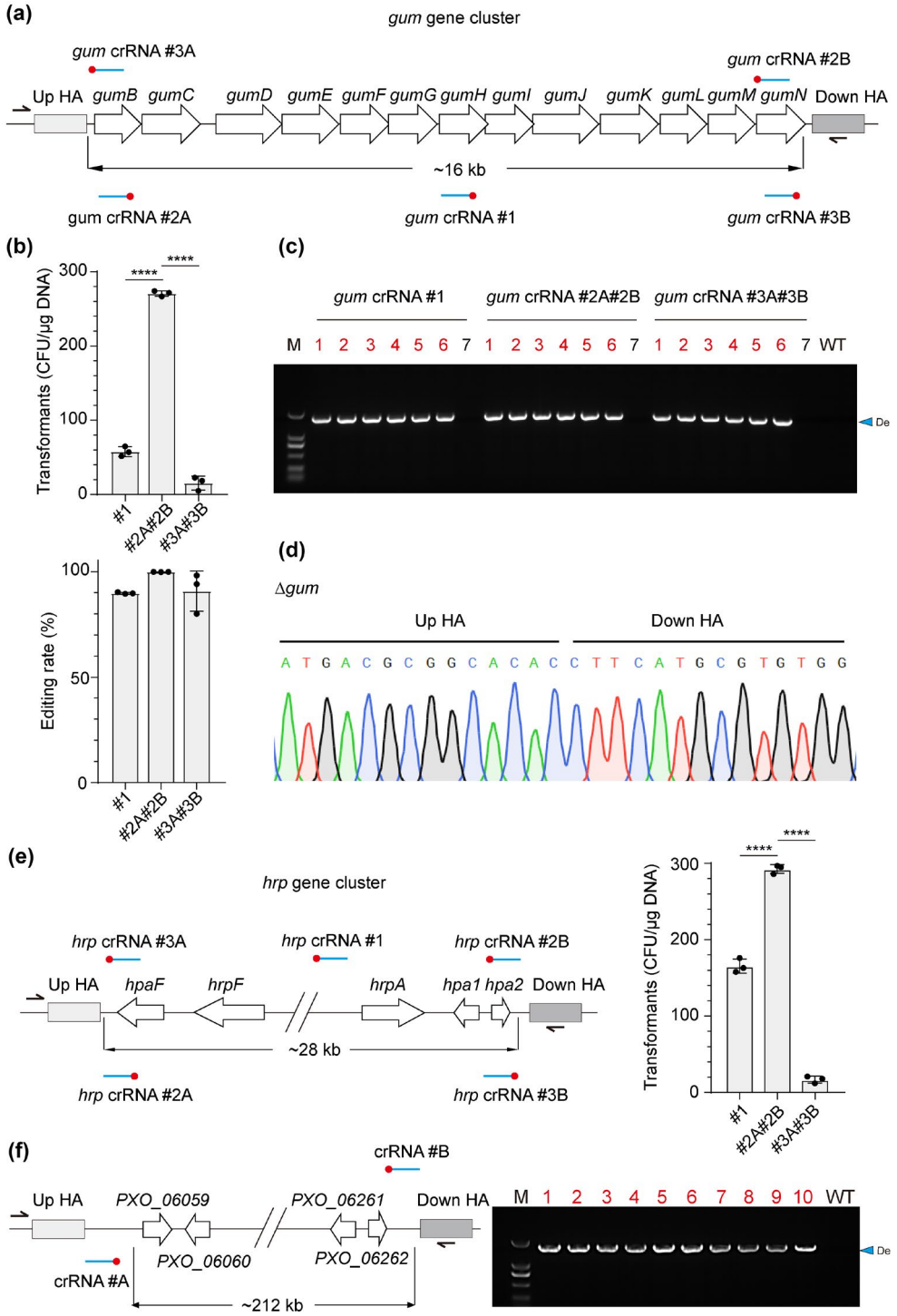

FIGURE 5 Large genomic deletions generated by harnessing the native type I-C CRISPR system in *Xanthomonas oryzae* pv. *oryzae*. (a) Schematic diagram for targeted deletion of the 16 kb *gum* gene cluster. The protospacers recognized by the selected crRNAs are in blue lines. Red dots denote the protospacer adjacent motif sequences. Pairs of half arrows in the figure indicate the target regions for the PCR amplification. (b) Transformant numbers (top) and editing rates (%) (bottom) achieved using various crRNAs. Error bars represent standard deviations, $n = 3$. Statistical significance was determined by one-way analysis of variance (****$p < 0.0001$). (c) Targeted PCR amplification confirmed the *gum* cluster deletion. Predicted size of the PCR products of the deletion mutants (De) is indicated by the blue triangle. Clone numbers with desired *gum* gene cluster deletion are highlighted in red and the clone numbers of escape colonies are in black. M, DNA size marker. (d) DNA sequencing confirmed successful deletion of the *gum* gene cluster. (e) Schematic diagram for 28 kb *hrp* gene cluster deletion and transformant numbers achieved using various crRNAs. Error bars represent standard deviations, $n = 3$. Statistical significance was determined by one-way analysis of variance (****$p < 0.0001$). (f) Schematic diagram and targeted PCR amplification result for the 212 kb region deletion. Predicted size of the PCR products of the deletion mutants (De) is indicated by the blue triangle

array together with repair templates, potentially due to the low frequency of homologous recombination in Xoo. Introduction of the λ-Red recombination system allowed for efficient genome editing mediated by enhancing recombination rates. We demonstrate that this optimized genome-editing system can generate base substitutions, insertions, and deletions, especially large deletions of up to 212 kb, at high efficiency and precision. This repurposed type I-C CRISPR system thus provides an efficient and accurate genome-engineering tool for this important plant pathogen.

The nonhomologous end-joining repair pathway is absent in Xoo, so repair of double-strand breaks introduced by CRISPR-directed chromosomal self-targeting relies on the homologous recombination pathway, which generally requires nonchromosomal templates carrying the desired mutation (Vento et al., 2019). Therefore, the length of DNA templates may also affect the editing efficiency in bacterial cells. We compared 500-bp and 1000-bp homologous arms on genome-editing efficiency. Although the 1000-bp homologous arms greatly increased the transformant amount (Figure S3d), the 500-bp repair arms were equally efficient for genome editing.

The double-crossover homologous recombination system has been widely applied in *Xanthomonas*, but the efficiency is still limited (Zou et al., 2011). After two rounds of crossover events, recombination will either restore the wild-type genotype or acquire the mutant allele in the chromosome, indicating a theoretical maximum mutagenesis rate of 50%. Furthermore, this double-crossover approach requires two rounds of selection, which is complicated and time-consuming. Our CRISPR-Cas system described here offers an efficient and easy approach for targeted genome editing in Xoo. We demonstrated that native homologous recombination is inefficient in Xoo cells (Figure 3a and Figure S2a), so the supplementation with the λ-Red recombination system greatly facilitates genome editing mediated by the endogenous type I-C CRISPR system.

The CRISPR-Cas system described here is also capable of achieving efficient large genomic deletions, which is difficult using classical genetic manipulation methods. Large genomic deletions can be obtained with high efficiencies in Xoo by using endogenous CRISPR-Cas systems attributed to the processive helicase-nuclease activity of Cas3. The largest deletion size achieved thus far can reach up to 212 kb. Therefore, type I-C CRISPR-based strategies offer a great tool for programmable large-scale genome engineering, such as the manipulation of repetitive and noncoding regions and genome minimization.

Further work can be carried out to develop more editing tools based on the endogenous type I-C CRISPR-Cas system in Xoo. Compared to other type I CRISPR systems, the type I-C is streamlined, requiring only four proteins to perform genome editing (Makarova et al., 2015). Furthermore, the minimal Cascade/I-C complex is composed of only three unique proteins, demonstrating the potential applicability of this system for heterologous editing in bacteria that do not naturally encode an endogenous CRISPR-Cas system. The type I-B, type I-E, and type I-F CRISPR systems have been harnessed for efficient transcriptional repression on the deletion of Cas3 (Luo et al., 2015; Stachler & Marchfelder, 2016; Zheng et al., 2019); therefore, we speculate that our type I-C CRISPR-Cas system may be repurposed for targeted transcriptional modulation and metabolic engineering in the future.

In summary, we present a new and optimized genome-editing tool that enables a variety of precise genetic manipulations in Xoo through repurposing the endogenous type I-C CRISPR system. This method will be essential to the study of plant innate immunity when using the critical rice–Xoo system as a model. Although we have focused on the plant pathogen Xoo, any active endogenous CRISPR-Cas system in other plant-pathogenic bacteria should be readily repurposed using a similar strategy. This strategy allows for efficient and diverse genetic manipulations, which will facilitate functional genomics studies of bacterial pathogens. Moreover, leveraging endogenous CRISPR systems outperforms conventional methods when engineering microorganisms because delivering multiple editing components and repair templates simultaneously to the same cell is very inefficient. We envision that the genome-editing system developed herein will have broad application in the study of host–pathogen interactions, microbiome engineering, and many other uses.

4 | EXPERIMENTAL PROCEDURES

4.1 | In silico identification and characterization of the native CRISPR-Cas system

The Xoo PXO99^{A} genome sequence is available in the National Center for Biotechnology Information (NCBI) GenBank (NCBI Reference Sequence: NC_010717.2). When the sequence was submitted to the CRISPRCasFinder website (https://crisprcas.i2bc.paris-saclay.fr/CrisprCasFinder/Index) (Grissa et al., 2007), one CRISPR-Cas locus was identified. The CRISPR type I-C subtype is defined by possession of a signature Cas protein and the constitution of the associated proteins, as previously reported (Nam et al., 2012). To predict the PAM sequences based on spacer-protospacer matching, the CRISPR array sequence was first submitted to the CRISPRTarget tool (http://bioanalysis.otago.ac.nz/CRISPRTarget/crispr_analysis.html) with default parameters (Biswas et al., 2013). The output from this initial prediction was considered as putative protospacers. The flanking regions of each protospacer were aligned and analysed by WebLogo (http://weblogo.berkeley.edu/logo.cgi) (Crooks et al., 2004) to determine the PAM preference.

4.2 | RNA sequencing analysis

Xoo PXO99^{A} was grown in liquid peptone sucrose (PS; 10 g/L tryptone, 10 g/L sucrose, 1 g/L glutamic acid, pH 7.0) medium to reach OD_{600} 0.6. Then the bacterial cells were collected and total RNA was extracted using a RiboPure Bacteria Kit (Thermo Fisher Scientific) following the manufacturer's instructions. The rRNA-depleted RNA was fragmented and reverse transcribed to cDNA for library

construction. The cDNA library was sequenced using an Illumina HiSeq X Ten platform with PE150 mode. Raw data were filtered by removing reads with adapters, reads with poly-N sequences, and reads of low-quality to obtain clean data. The clean reads were then mapped to the Xoo genome using Geneious Prime software with default settings (Kearse et al., 2012). The expression levels for *cas* genes were calculated based on the fragments per kilobase per million reads (FPKM) values.

4.3 | Bacterial strains and growth conditions

Xoo PXO99^A and derivative strains employed in this study are listed in Table S2. Bacteria were grown in PS medium or on PS agar (PSA) plates containing suitable antibiotics at 28°C for 3 days (Tsuchiya et al., 1982). *Escherichia coli* DH5α was used for plasmid culture and grown in Luria Bertani medium on 1.5% agar plates at 37°C, supplemented with spectinomycin (100 μg/ml) or gentamicin (50 μg/ml).

4.4 | Plasmid construction

For the plasmid interference assay, we chose spacer 1 of the native CRISPR array in Xoo as the protospacer sequence to combine with different PAM sequences. A pair of complementary oligonucleotides corresponding to each PAM-protospacer1 combination was synthesized with a desired 4-nucleotide 5′-overhang introduced to each oligonucleotide. The complementary oligonucleotides were annealed and then ligated into *Eco*RI/*Hin*dIII sites of pHM1 vector to yield the interference plasmids pHM1-PAM(s).

To increase the frequency of homologous recombination, the phage-derived recombination system λ-Red under the control of the P_{araB} promoter, which is induced by L-arabinose, was inserted by Gibson assembly into *Kpn*I/*Hin*dIII-digested pHM1 vector to yield pHM1-λRed.

For gene targeting, pSEVA-gRic6T (Sun et al., 2018) was modified by adding two repeat sequences separated by two *Bsa*I sites yielding pSEVA-xT ("x" represents the name of targeted gene), and the synthetic constitutive promoter *J23119* was retained. Then spacer fragments were generated by annealing of complementary oligonucleotides and inserted into pSEVA-xT at the *Bsa*I sites by Golden Gate cloning, yielding a plasmid carrying an artificial mini-CRISPR array.

For genome editing, 500-bp or 1000-bp sequences upstream and downstream of the target gene were individually amplified and connected via overlap-PCR. The resulting homologous DNA fragment was then inserted into *Bam*HI/*Hin*dIII-digested pSEVA-xT by Gibson assembly, yielding pSEVA-xTD.

The reaction products were then transformed into *E. coli* DH5α cells with selection using suitable antibiotics. All final plasmids were confirmed by Sanger sequencing (RuiBiotech). All oligonucleotides were synthesized by BGI and restriction enzymes were purchased from NEB. All the primers used in this work are listed in Table S3.

4.5 | Transformation of Xoo

Plasmids were transformed into Xoo PXO99^A by electroporation. First, strains stored at −80 °C were streaked on PSA plates and cultured at 28°C for 2–3 days. Next, a single Xoo colony was selected and cultivated in 5 ml of liquid M210 medium (8 g/L casein enzymatic hydrolysate, 5 g/L sucrose, 4 g/L yeast extract, 17.2 mM K_2HPO_4, 1.2 mM $MgSO_4.7H_2O$, pH 7.0) at 28°C and 220 rpm overnight, then transferred to a 1 L flask containing 250 ml of M210 to OD_{600} 0.5–0.6. After concentration, electrocompetent cells were prepared by three washes in ice-cold 10% glycerol. Finally, the cells were resuspended in 1 ml of ice-cold 10% glycerol (vol/vol) and split into 100-μl aliquots for direct use. For electroporation, 100 μl of bacterial suspension and plasmid DNA were transferred to a 1-mm gap ice-cold electroporation cup and electroporated using a Bio-Rad MicroPulser. After electroporation, 900 μl of PS medium was added and the mixture was transferred into a 1.5-ml Eppendorf tube and incubated at 28°C for 4 h before being spread on PSA selection plates.

For interference assays, 1 ng of pHM1-PAM(s) plasmid was used for transformation. For genome editing, first the auxiliary pHM1-λRed vector was introduced into wild-type PXO99^A by electroporation, yielding PXO99$^A_{\lambda Red}$ cells as the basic strain. Second, these cells were grown to OD_{600} 0.2–0.3, 10 mM L-arabinose was added, and the cells were grown further to OD_{600} 0.5–0.6 and harvested. Finally, 2 μg pSEVA-derived plasmid was transformed into the PXO99$^A_{\lambda Red}$ competent cells by electroporation and the cells were plated on PSA plates with spectinomycin (100 μg/ml) and gentamicin (50 μg/ml) for 3 days.

4.6 | Mutant screening

DNA was extracted from single colonies with a TIANamp Bacteria Kit (Tiangen) and tested by PCR for the wild-type target gene and mutated alleles using the primers listed in Table S3. The resulting PCR products were analysed by agarose gel electrophoresis and sequenced to confirm the presence of the desired mutation (RuiBiotech).

4.7 | Pathogen virulence assay

Virulence was assayed by the leaf-tip clipping method (Yang & Bogdanove, 2013). Briefly, bacterial cells were washed twice in 10 mM $MgCl_2$ and OD_{600} adjusted to 0.5. The two most recent fully expanded leaves of rice seedlings at the six-leaf stage were clipped about 2 cm from the tip, then immersed in the bacterial suspension. Lesion lengths on individual leaves were measured 12 days after inoculation.

ACKNOWLEDGEMENTS

This study was supported by the Strategic Priority Research Program of the Chinese Academy of Sciences (XDA24020101, XDPB16)

and the National Natural Science Foundation of China (32001891, 31901868).

DATA AVAILABILITY STATEMENT

The RNA-Seq data are available in the NCBI BioProject database at https://www.ncbi.nlm.nih.gov/bioproject/ with accession code PRJNA783485. The data that support the findings of this study are available from the corresponding author upon reasonable request.

ORCID

Jin-Long Qiu https://orcid.org/0000-0001-8054-2552

REFERENCES

Anzalone, A.V., Koblan, L.W. & Liu, D.R. (2020) Genome editing with CRISPR–Cas nucleases, base editors, transposases and prime editors. *Nature Biotechnology*, 38, 824–844.

Arroyo-Olarte, R.D., Bravo Rodríguez, R. & Morales-Ríos, E. (2021) Genome editing in bacteria: CRISPR-Cas and beyond. *Microorganisms*, 9, 844.

Baker, P.L., Orf, G.S., Kevershan, K., Pyne, M.E., Bicer, T. & Redding, K.E. (2019) Using the endogenous CRISPR-Cas system of *Heliobacterium modesticaldum* to delete the photochemical reaction center core subunit gene. *Applied and Environmental Microbiology*, 85, e01644-19.

Biswas, A., Gagnon, J.N., Brouns, S.J.J., Fineran, P.C. & Brown, C.M. (2013) CRISPRTarget: bioinformatic prediction and analysis of crRNA targets. *RNA Biology*, 10, 817–827.

Chen, X. & Ronald, P.C. (2011) Innate immunity in rice. *Trends in Plant Science*, 16, 451–459.

Cheng, F., Gong, L., Zhao, D., Yang, H., Zhou, J., Li, M. et al. (2017) Harnessing the native type I-B CRISPR-Cas for genome editing in a polyploid archaeon. *Journal of Genetics and Genomics*, 44, 541–548.

Cornelis, G.R. (2006) The type III secretion injectisome. *Nature Reviews Microbiology*, 4, 811–825.

Crooks, G.E., Hon, G., Chandonia, J.M. & Brenner, S.E. (2004) WebLogo: a sequence logo generator. *Genome Research*, 14, 1188–1190.

Datsenko, K.A. & Wanner, B.L. (2000) One-step inactivation of chromosomal genes in *Escherichia coli* K-12 using PCR products. *Proceedings of the National Academy of Sciences of the United States of America*, 97, 6640–6645.

Dolan, A.E., Hou, Z., Xiao, Y., Gramelspacher, M.J., Heo, J., Howden, S.E. et al. (2019) Introducing a spectrum of long-range genomic deletions in human embryonic stem cells using type I CRISPR-Cas. *Molecular Cell*, 74, 936–950.e5.

Grissa, I., Vergnaud, G. & Pourcel, C. (2007) CRISPRFinder: a web tool to identify clustered regularly interspaced short palindromic repeats. *Nucleic Acids Research*, 35, W52–W57.

Guzman, L.M., Belin, D., Carson, M.J. & Beckwith, J. (1995) Tight regulation, modulation, and high level expression by vectors containing the arabinose PBAD promoter. *Journal of Bacteriology*, 177, 4121–4130.

Hmelo, L.R., Borlee, B.R., Almblad, H., Love, M.E., Randall, T.E., Tseng, B.S. et al. (2015) Precision-engineering the *Pseudomonas aeruginosa* genome with two-step allelic exchange. *Nature Protocols*, 10, 1820–1841.

Hochstrasser, M.L., Taylor, D.W., Kornfeld, J.E., Nogales, E. & Doudna, J.A. (2016) DNA targeting by a minimal CRISPR RNA-guided cascade. *Molecular Cell*, 63, 840–851.

Hong, W., Zhang, J., Cui, G., Wang, L. & Wang, Y. (2018) Multiplexed CRISPR-Cpf1-mediated genome editing in *Clostridium difficile* toward the understanding of pathogenesis of *C. difficile* infection. *ACS Synthetic Biology*, 7, 1588–1600.

Hopkins, C.M., White, F.F., Choi, S.H., Guo, A. & Leach, J.E. (1992) Identification of a family of avirulence genes from *Xanthomonas oryzae* pv. *oryzae*. *Molecular Plant-Microbe Interactions*, 5, 451–459.

Innes, R.W., Hirose, M.A. & Kuempel, P.L. (1988) Induction of nitrogen-fixing nodules on clover requires only 32 kilobase pairs of DNA from the *Rhizobium trifolii* symbiosis plasmid. *Journal of Bacteriology*, 170, 3793–3802.

Jiang, N., Yan, J., Liang, Y.I., Shi, Y., He, Z., Wu, Y. et al. (2020) Resistance genes and their interactions with bacterial blight/leaf streak pathogens (*Xanthomonas oryzae*) in rice (*Oryza sativa* L.) – an updated review. *Rice*, 13, 3.

Jiang, W., Bikard, D., Cox, D., Zhang, F. & Marraffini, L.A. (2013) RNA-guided editing of bacterial genomes using CRISPR-Cas systems. *Nature Biotechnology*, 31, 233–239.

Jiang, Y., Chen, B., Duan, C., Sun, B., Yang, J. & Yang, S. (2015) Multigene editing in the *Escherichia coli* genome via the CRISPR-Cas9 system. *Applied and Environmental Microbiology*, 81, 2506–2514.

Joshi, J.B., Arul, L., Ramalingam, J. & Uthandi, S. (2020) Advances in the Xoo–rice pathosystem interaction and its exploitation in disease management. *Journal of Biosciences*, 45, 112.

Katzen, F., Ferreiro, D.U., Oddo, C.G., Ielmini, M.V., Becker, A., Puhler, A. et al. (1998) *Xanthomonas campestris* pv. *campestris gum* mutants: effects on xanthan biosynthesis and plant virulence. *Journal of Bacteriology*, 180, 1607–1617.

Kearse, M., Moir, R., Wilson, A., Stones-Havas, S., Cheung, M., Sturrock, S. et al. (2012) Geneious Basic: an integrated and extendable desktop software platform for the organization and analysis of sequence data. *Bioinformatics*, 28, 1647–1649.

Kessler, A., Brinkman, A.B., van der Oost, J. & Prangishvili, D. (2004) Transcription of the rod-shaped viruses SIRV1 and SIRV2 of the hyperthermophilic archaeon *Sulfolobus*. *Journal of Bacteriology*, 186, 7745–7753.

Kim, S.Y., Kim, J.G., Lee, B.M. & Cho, J.Y. (2009) Mutational analysis of the *gum* gene cluster required for xanthan biosynthesis in *Xanthomonas oryzae* pv. *oryzae*. *Biotechnology Letters*, 31, 265–270.

Leenay, R., Maksimchuk, K., Slotkowski, R., Agrawal, R., Gomaa, A., Briner, A. et al. (2016) Identifying and visualizing functional PAM diversity across CRISPR-Cas systems. *Molecular Cell*, 62, 137–147.

Li, Y., Pan, S., Zhang, Y., Ren, M., Feng, M., Peng, N. et al. (2016) Harnessing type I and type III CRISPR-Cas systems for genome editing. *Nucleic Acids Research*, 44, e34.

Liu, W., Liu, J., Triplett, L., Leach, J.E. & Wang, G.L. (2014) Novel insights into rice innate immunity against bacterial and fungal pathogens. *Annual Review of Phytopathology*, 52, 213–241.

Luo, M.L., Mullis, A.S., Leenay, R.T. & Beisel, C.L. (2015) Repurposing endogenous type I CRISPR-Cas systems for programmable gene repression. *Nucleic Acids Research*, 43, 674–681.

Maikova, A., Kreis, V., Boutserin, A., Severinov, K. & Soutourina, O. (2019) Using an endogenous CRISPR-Cas system for genome editing in the human pathogen *Clostridium difficile*. *Applied and Environmental Microbiology*, 85, e01416-19.

Makarova, K.S., Wolf, Y.I., Alkhnbashi, O.S., Costa, F., Shah, S.A., Saunders, S.J. et al. (2015) An updated evolutionary classification of CRISPR-Cas systems. *Nature Reviews Microbiology*, 13, 722–736.

Makarova, K.S., Wolf, Y.I. & Koonin, E.V. (2018) Classification and nomenclature of CRISPR-Cas systems: where from here? *The CRISPR Journal*, 1, 325–336.

Mansfield, J., Genin, S., Magori, S., Citovsky, V., Sriariyanum, M., Ronald, P. et al. (2012) Top 10 plant pathogenic bacteria in molecular plant pathology. *Molecular Plant Pathology*, 13, 614–629.

Martins, P.M.M., da Silva Xavier, A., Takita, M.A., Alfemas-Zerbini, P. & de Souza, A.A. (2019) CRISPR-Cas systems in the plant pathogen *Xanthomonas* spp. and their impact on genome plasticity. *bioRxiv*. https://doi.org/10.1101/731166

Mew, T.W., Alvarez, A.M., Leach, J.E. & Swings, J. (1993) Focus on bacterial blight of rice. *Plant Disease*, 77, 5–12.

Mojica, F.J.M., Diez-Villasenor, C., Garcia-Martinez, J. & Almendros, C. (2009) Short motif sequences determine the targets of the prokaryotic CRISPR defence system. *Microbiology*, 155, 733–740.

Mulepati, S. & Bailey, S. (2013) In vitro reconstitution of an *Escherichia coli* RNA-guided immune system reveals unidirectional, ATP-dependent degradation of DNA target. *Journal of Biological Chemistry*, 288, 22184–22192.

Nam, K., Haitjema, C., Liu, X., Ding, F., Wang, H., DeLisa, M. et al. (2012) Cas5d protein processes pre-crRNA and assembles into a cascade-like interference complex in subtype I-C/Dvulg CRISPR-Cas system. *Structure*, 20, 1574–1584.

Nguyen, M.P., Park, J., Cho, M.H. & Lee, S.W. (2016) Role of DetR in defence is critical for virulence of *Xanthomonas oryzae* pv. *oryzae*. *Molecular Plant Pathology*, 17, 601–613.

Nimkar, S. & Anand, B. (2020) Cas3/I-C mediated target DNA recognition and cleavage during CRISPR interference are independent of the composition and architecture of Cascade surveillance complex. *Nucleic Acids Research*, 48, 2486–2501.

Niño-Liu, D.O., Ronald, P.C. & Bogdanove, A.J. (2006) *Xanthomonas oryzae* pathovars: model pathogens of a model crop. *Molecular Plant Pathology*, 7, 303–324.

Penewit, K., Holmes, E.A., McLean, K., Ren, M., Waalkes, A. & Salipante, S.J. (2018) Efficient and scalable precision genome editing in Staphylococcus aureus through conditional recombineering and CRISPR/Cas9-mediated counterselection. *mBio*, 9, e00067-18.

Pyne, M.E., Bruder, M.R., Moo-Young, M., Chung, D.A. & Chou, C.P. (2016) Harnessing heterologous and endogenous CRISPR-Cas machineries for efficient markerless genome editing in *Clostridium*. *Scientific Reports*, 6, 25666.

Rao, C., Guyard, C., Pelaz, C., Wasserscheid, J., Bondy-Denomy, J., Dewar, K. et al. (2016) Active and adaptive *Legionella* CRISPR-Cas reveals a recurrent challenge to the pathogen. *Cellular Microbiology*, 18, 1319–1338.

Rocha, E.P.C., Cornet, E. & Michel, B. (2005) Comparative and evolutionary analysis of the bacterial homologous recombination systems. *PLoS Genetics*, 1, e15.

Salzberg, S.L., Sommer, D.D., Schatz, M.C., Phillippy, A.M., Rabinowicz, P.D., Tsuge, S. et al. (2008) Genome sequence and rapid evolution of the rice pathogen *Xanthomonas oryzae* pv. *oryzae* PXO99^{A}. *BMC Genomics*, 9, 204.

Savary, S., Willocquet, L., Pethybridge, S.J., Esker, P., McRoberts, N. & Nelson, A. (2019) The global burden of pathogens and pests on major food crops. *Nature Ecology and Evolution*, 3, 430–439.

Schäfer, A., Tauch, A., Jäger, W., Kalinowski, J., Thierbach, G. & Pühler, A. (1994) Small mobilizable multi-purpose cloning vectors derived from the *Escherichia coli* plasmids pK18 and pK19: selection of defined deletions in the chromosome of *Corynebacterium glutamicum*. *Gene*, 145, 69–73.

Sinkunas, T., Gasiunas, G., Fremaux, C., Barrangou, R., Horvath, P. & Siksnys, V. (2011) Cas3 is a single-stranded DNA nuclease and ATP-dependent helicase in the CRISPR/Cas immune system. *The EMBO Journal*, 30, 1335–1342.

Sinkunas, T., Gasiunas, G., Waghmare, S.P., Dickman, M.J., Barrangou, R., Horvath, P. et al. (2013) In vitro reconstitution of Cascade-mediated CRISPR immunity in *Streptococcus thermophilus*. *The EMBO Journal*, 32, 385–394.

Stachler, A.E. & Marchfelder, A. (2016) Gene repression in Haloarchaea using the CRISPR (clustered regularly interspaced short palindromic repeats)-Cas I-B system. *Journal of Biological Chemistry*, 291, 15226–15242.

Sun, J., Wang, Q., Jiang, Y.U., Wen, Z., Yang, L., Wu, J. et al. (2018) Genome editing and transcriptional repression in *Pseudomonas putida* KT2440 via the type II CRISPR system. *Microbial Cell Factories*, 17, 41.

Sun, Q., Wu, W., Qian, W., Hu, J., Fang, R. & He, C. (2003) High-quality mutant libraries of *Xanthomonas oryzae* pv. *oryzae* and *X. campestris* pv. *campestris* generated by an efficient transposon mutagenesis system. *FEMS Microbiology Letters*, 226, 145–150.

Todor, H., Silvis, M.R., Osadnik, H. & Gross, C.A. (2021) Bacterial CRISPR screens for gene function. *Current Opinion in Microbiology*, 59, 102–109.

Tsuchiya, K., Mew, T.W. & Wakimoto, S. (1982) Bacteriological and pathological characteristics of wild types and induced mutants of *Xanthomonas campestris* pv. *oryzae*. *Phytopathology*, 72, 43–46.

Vento, J.M., Crook, N. & Beisel, C.L. (2019) Barriers to genome editing with CRISPR in bacteria. *Journal of Industrial Microbiology and Biotechnology*, 46, 1327–1341.

Verdier, V., Vera Cruz, C. & Leach, J.E. (2012) Controlling rice bacterial blight in Africa: needs and prospects. *Journal of Biotechnology*, 159, 320–328.

Wang, J.C., So, B.H., Kim, J.H., Park, Y.J., Lee, B.M. & Kang, H.W. (2008) Genome-wide identification of pathogenicity genes in *Xanthomonas oryzae* pv. *oryzae* by transposon mutagenesis. *Plant Pathology*, 57, 1136–1145.

Xu, Z., Li, M., Li, Y., Cao, H., Miao, L., Xu, Z. et al. (2019) Native CRISPR-Cas-mediated genome editing enables dissecting and sensitizing clinical multidrug-resistant *P. aeruginosa*. *Cell Reports*, 29, 1707–1717.

Xu, Z., Li, Y., Cao, H., Si, M., Zhang, G., Woo, P.C.Y. et al. (2021) A transferrable and integrative type I-F Cascade for heterologous genome editing and transcription modulation. *Nucleic Acids Research*, 49, e94.

Yang, B. & Bogdanove, A. (2013) Inoculation and virulence assay for bacterial blight and bacterial leaf streak of rice. *Methods in Molecular Biology*, 956, 249–255.

Yoon, K.H. & Cho, J.Y. (2007) Transcriptional analysis of the *gum* gene cluster from *Xanthomonas oryzae* pathovar *oryzae*. *Biotechnology Letters*, 29, 95–103.

Zhang, D., Tian, C., Yin, K., Wang, W. & Qiu, J.L. (2019) Postinvasive bacterial resistance conferred by open stomata in rice. *Molecular Plant-Microbe Interactions*, 32, 255–266.

Zheng, Y., Han, J., Wang, B., Hu, X., Li, R., Shen, W. et al. (2019) Characterization and repurposing of the endogenous Type I-F CRISPR-Cas system of *Zymomonas mobilis* for genome engineering. *Nucleic Acids Research*, 47, 11461–11475.

Zhou, L., Wang, J.-Y., Wang, J., Poplawsky, A., Lin, S., Zhu, B. et al. (2013) The diffusible factor synthase XanB2 is a bifunctional chorismatase that links the shikimate pathway to ubiquinone and xanthomonadins biosynthetic pathways. *Molecular Microbiology*, 87, 80–93.

Zhu, W.G., Magbanua, M.M. & White, F.F. (2000) Identification of two novel hrp-associated genes in the *hrp* gene cluster of *Xanthomonas oryzae* pv. *oryzae*. *Journal of Bacteriology*, 182, 1844–1853.

Zou, L., Li, Y. & Chen, G. (2011) A non-marker mutagenesis strategy to generate poly-*hrp* gene mutants in the rice pathogen *Xanthomonas oryzae* pv. *oryzicola*. *Agricultural Sciences in China*, 10, 1139–1150.

SUPPORTING INFORMATION

Additional supporting information may be found in the online version of the article at the publisher's website.

How to cite this article: Jiang, D., Zhang, D., Li, S., Liang, Y., Zhang, Q., Qin, X. et al. (2022) Highly efficient genome editing in *Xanthomonas oryzae* pv. *oryzae* through repurposing the endogenous type I-C CRISPR-Cas system. *Molecular Plant Pathology*, 23, 583–594. https://doi.org/10.1111/mpp.13178